

# Optical to IRAS galaxy bias factor using the Local Group Dipole

M. Plionis<sup>1</sup> & S. Basilakos<sup>1,2</sup>

<sup>1</sup> *Astronomical Institute, National Observatory of Athens,  
I.Metaxa & Bas.Pavlou, Lofos Koufou, 15236, Athens, Greece*

<sup>2</sup> *Section of Astronomy & Astrophysics, Univ. of Athens,  
Panepistimioupolis, 15784 Zografos, Athens, Greece*

Comparing the gravitational acceleration induced on the Local Group by optical (SSRS2; da Costa et al 1994, 1998) and IRAS (1.2 Jy; Fisher et al 1995 and 0.6 Jy - QDOT; Rowan-Robinson et al 1990) galaxies we estimate, within the framework of linear theory, their relative bias factor. Using both IRAS samples we find  $\mathbf{b}_{\text{OI}} \approx 1.14 - 1.2$ , slightly lower than in Willmer, Da Costa & Pellegrini (1998) who use a  $\xi(r)$  approach.

Using linear perturbation theory one can relate the gravitational acceleration induced on the observer by the surrounding mass distribution to her/his peculiar velocity:

$$\mathbf{u}(\mathbf{r}) = \frac{\Omega_{\circ}^{0.6}}{b} \frac{1}{4\pi} \int \delta(\mathbf{r}) \frac{\mathbf{r}}{|\mathbf{r}|^3} d\mathbf{r} = \frac{\Omega_{\circ}^{0.6}}{b} \mathbf{D}(r)$$

where

$$\mathbf{D} = \frac{1}{4\pi\bar{n}} \sum_{i=1}^N \frac{1}{\phi_i r_i^2} \hat{\mathbf{r}}_i$$

with  $\phi(r) = \langle n \rangle^{-1} \int_{L_{\min}(r)}^{L_{\max}} \Phi(L) dL$ , where  $\Phi(L)$  is the luminosity function of the objects under study and  $L_{\min}(r) = 4\pi r^2 S_{\text{lim}}$ , with  $S_{\text{lim}}$  being the flux limit of the sample under study.

Different classes of extragalactic objects (QSOs, AGNs, galaxies, clusters of galaxies) trace differently the underlying matter distribution, usually assumed to be linearly related via  $(\delta\rho/\rho)_{\text{tracer}} = b_{\text{tracer,m}} (\delta\rho/\rho)_{\text{mass}}$  (cf. Kaiser 1984). Although this complicates the use of dipole as an estimator of the cosmological density parameter,  $\Omega_{\circ}$ , it does allow one in principle to study the relative bias displayed by such objects (Kolokotronis *et al* 1996; Plionis 1995).

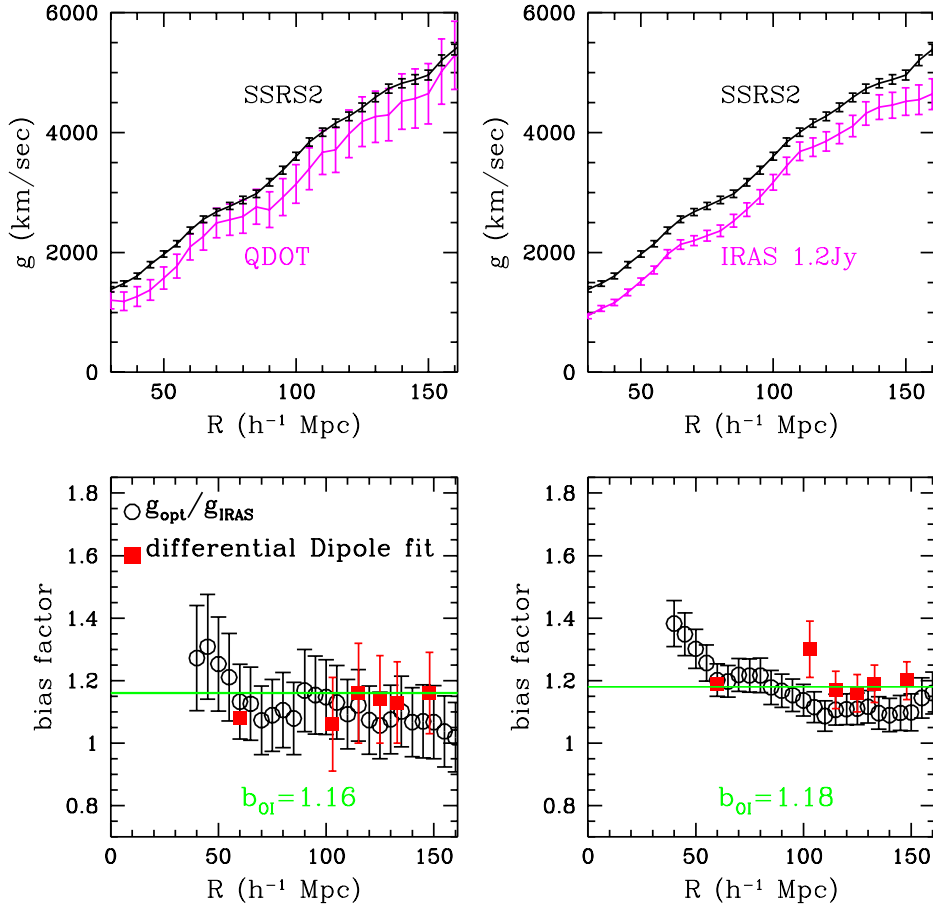
Using different tracers, ie. SSRS2 optical and IRAS galaxies, to determine the Local Group acceleration (dipole) we can write:  $\mathbf{u}(\mathbf{r}) = \Omega_c^{0.6} \mathbf{D}_o(r)/b_o = \Omega_c^{0.6} \mathbf{D}_I(r)/b_I$  and therefore we can obtain an estimate of their relative bias factor from:

$$b_{OI} = \frac{b_o}{b_I} = \frac{\mathbf{D}_o(r)}{\mathbf{D}_I(r)} \left( \equiv \frac{\mathbf{g}_o(r)}{\mathbf{g}_I(r)} \right)$$

A statistically more reliable approach is to use the differential dipole, estimated in equal volume shells, to fit  $b_{OI}$  according to:

$$\chi^2 = \sum_{i=1}^{N_{bins}} \frac{(\mathbf{D}_{o,i} - b_{OI} \mathbf{D}_{I,i} - C_i)^2}{\sigma_{o,i}^2 + b_{OI}^2 \sigma_{I,i}^2}$$

where  $C$  is the zero-point offset of the relation and  $\sigma$  are the corresponding shot-noise errors estimated according to Strauss et al. (1992).



In the figure and in table 1 we present the results of both methods used to estimate the optical (SSRS2) to infrared (IRAS 1.2 Jy and QDOT) bias factors.

Table 1: Optical to Infrared galaxy bias factors from differential dipole fit.

samples	$b_{OI}$	$C$	$\chi^2$	d.f.
SSRS2-QDOT	<b><math>1.16 \pm 0.13</math></b>	$-80 \pm 70$	8.7	6
SSRS2-IRAS 1.2 Jy	<b><math>1.18 \pm 0.06</math></b>	$-30 \pm 30$	15.7	6

## References

- da Costa, L.N. *et al.*, 1994, ApJ, 424, L1  
da Costa, L.N. *et al.*, 1998, *in preparation*  
Fisher, K.B., Huchra, J.P., Strauss, M.A., Davis, M., Yahil, A. & Schlegel, D., 1995, ApJS, 100, 69  
Kaiser N., 1984, ApJ, 284, L9  
Kolokotronis, V. *et al.*, 1996, MNRAS, 280, 186  
Plionis, M., 1995, in Balkowsky C. *et al*, eds, Proc. of the Moriond Astrophysics Meeting on Clustering in the Universe, Editions Frontieres.  
Rowan-Robinson M., *et al.*, 1990, MNRAS, 247, 1  
Strauss M., Yahil A., Davis M., Huchra J.P., Fisher K., 1992 ApJ, 397, 395  
Willmer, C.N.A., Da Costa, L.N. & Pellegrini, P.S., 1998, *astro-ph/9803118*

# The X-ray Luminosity Function of Local Galaxies

S. Basilakos<sup>1,2</sup>, I. Georgantopoulos<sup>1</sup>, M. Plionis<sup>1</sup>, O. Giannakis<sup>1</sup>

<sup>1</sup> Astronomical Institute, National Observatory of Athens,  
I.Metaxa & Bas.Pavlou, Lofos Koufou, 15236, Athens, Greece

<sup>2</sup> Section of Astronomy & Astrophysics, Univ. of Athens,  
Panepistimioupolis, 15784 Zografos, Athens, Greece

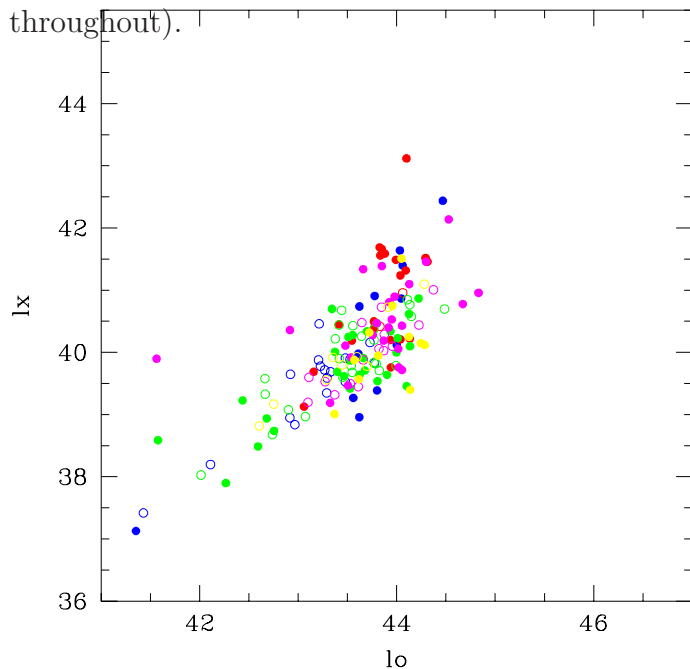
We construct the X-ray luminosity (LF) for different classes of galaxies (Seyferts, ellipticals, star-forming galaxies and Liners), by convolving the optical LF of the Ho *et al.* spectroscopic sample of nearby galaxies with the corresponding  $L_x/L_o$  relations from the Fabbiano et al. X-ray atlas of galaxies. From the derived LF we can easily assess the contribution of galaxies to the X-ray background. The **Seyferts and Liners make the largest contribution ( $\sim 40\%$ ) assuming no evolution** while the contribution of star-forming galaxies is much smaller ( $\sim 5\%$ ).

## The Sample & Method

We have used the spectroscopic sample of nearby galaxies ( $B < 12.5$ ) of Ho *et al.* (1995). The great advantage of this sample is that there is excellent spectroscopic information (high signal-to-noise, medium resolution) available and thus bona-fide spectroscopic identifications exist for all ( $\sim 500$ ) galaxies in the sample. Hence, we can construct the X-ray LF separately for Seyferts, star-forming galaxies (HII), ellipticals and Liners instead of simply dividing them to early-type and late-type according to their morphology. The majority of galaxies in the Ho *et al.* sample are **HII (50%), Liners are (30%), Seyferts (13%)** while **15% of galaxies present no emission lines** and thus can be classified as 'early-type' galaxies or 'ellipticals' on the basis of their spectra rather than their morphology (Ho *et al.* 1997). We first derive the optical LF for different classes of objects (Seyferts, HII, Liners and no-emission-line or early-type galaxies) using the classical  $1/V_{max}$  method. Next, we derive the  $L_x/L_B$  relation for the different subclasses using the EINSTEIN X-ray fluxes (0.5-4.0 keV) from the Fabbiano et al. (1992) X-ray atlas of galaxies. There are 164 entries (95 detections and 69  $3\sigma$  upper limits) of Ho et al. galaxies in the Fabbiano atlas. Finally, in order to derive the X-ray LF we convolve the optical LF with the  $L_x/L_B$  relation:

$$\Phi(L_x) = \int \Phi(L_B)\phi(L_x|L_B)dL_B$$

(eg Avni & Tananbaum 1986), where  $\phi(L_x|L_B)$  is the conditional probability function and can be expressed as a Gaussian around the mean  $L_x$  value for a given  $L_B$  (we use  $H_o = 100$  throughout).



Although, our method provides only an indirect way of deriving the X-ray LF, it is currently the only feasible method at least for some classes of galaxies. Unfortunately, the galaxies in X-rays are faint (apart from Seyferts) and thus we cannot yet obtain large X-ray selected galaxy samples neither in deep X-ray surveys nor in the ROSAT all-sky survey. For example we note that there are only 5 HII galaxies from the Ho et al. sample detected by the RASS (Zezas *et al.* 1998).

### The Results

In the figure we plot the X-ray luminosities vs. the Blue luminosities ( $\log_{10}(L_x)$  vs  $\log_{10}(L_B)$ ), for different subclasses (open symbols represent upper limits while filled symbols represent detections; the color coding is as in the table).

The X-ray LF is plotted on Fig. 2. It is clear that although the HII galaxies are the most numerous, due to their low  $L_*$  they contribute much less X-ray luminosity per  $h^{-3} \text{ Mpc}^3$  compared to Seyfert galaxies. Indeed, the HII emissivity is  $J \sim 1 \times 10^{38} \text{ erg s}^{-1} h^3 \text{ Mpc}^{-3}$

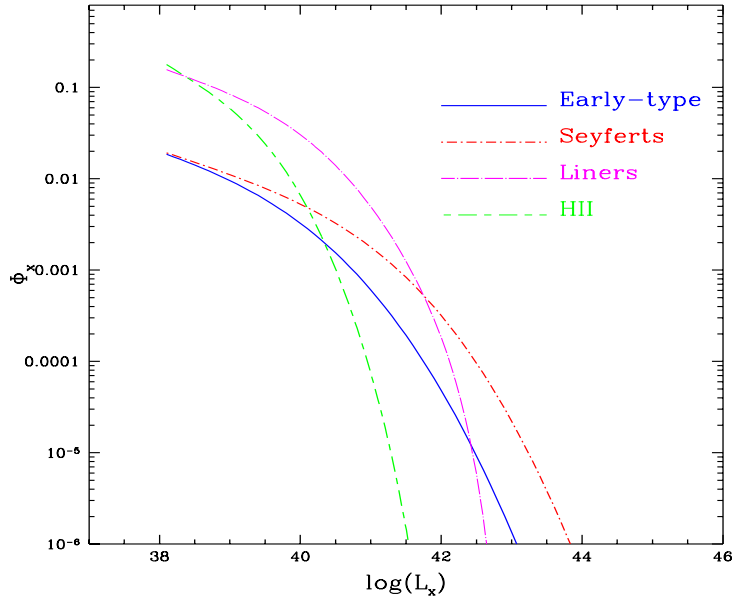


Table 2: The best-fit  $\Phi_x$  results for a Schechter optical luminosity function

Type	$\Phi_*$	$\alpha$	$M_*$	$\chi^2/dof$
Seyferts	0.001	$-1.39^{+0.350}_{-0.460}$	$-20.09^{+0.290}_{-0.130}$	0.250
LINER	0.005	$-1.19^{+0.230}_{-0.320}$	$-19.77^{+0.200}_{-0.290}$	0.646
HII	0.005	$-1.39^{+0.154}_{-0.088}$	$-19.75^{+0.240}_{-0.376}$	1.000
early-type	0.002	$-1.39^{+0.380}_{-0.560}$	$-19.73^{+0.290}_{-0.370}$	1.622
All	0.016	$-1.29^{+0.040}_{-0.130}$	$-19.70^{+0.047}_{-0.500}$	1.970

while the Seyfert is  $J \sim 8 \times 10^{38} \text{ erg s}^{-1} \text{ h}^3 \text{ Mpc}^{-3}$ . The total galaxy emissivity is comparable to the emissivity of local galaxies in the 2-10 keV band derived by Lahav et al. (1993) from the cross-correlation of optical galaxy catalogues with the fluctuations of the hard X-ray background.

## References

- [1] Avni, Y., Tananbaum, H., 1986, ApJ, 305, 83
- [2] Fabbiano, G., Kim, D.W., Trinchieri, G., 1992, ApJS, 80, 531
- [3] Ho, L.C. Filippenko, A.V., Sargent, W.L., 1995, ApJS, 98, 477

[4] Ho, L.C., Filippenko, A.V., Sargent, W.L., 1997, ApJ, 487, 568

[5] Lahav, O. et al. 1993, Nature, 364, 693

[6] Zezas, A., Georgantopoulos, I. Ward, M.J., 1998, Astron. Astroph. Tran., in press

# The ROSAT X-ray Background Dipole

M. Plionis & I. Georgantopoulos

Astronomical Institute, National Observatory of Athens,  
I.Metaxa & Bas.Pavlou, Lofos Koufou, 15236, Athens, Greece

We estimate the dipole of the diffuse 1.5 keV X-ray background from the ROSAT all-sky survey map of Snowden et al (1995). We first subtract the diffuse Galactic emission by fitting to the data a finite disk model, following Iwan et al (1982). We further exclude regions of low galactic latitudes, of local X-ray emission (eg the North Polar Spur) and model them using two different methods. We find that the ROSAT X-ray background dipole points towards  $(\mathbf{l}, \mathbf{b}) \approx (288^\circ, 25^\circ) \pm 19^\circ$  within  $\sim 30^\circ$  of the CMB; its direction is also in good agreement with the HEAO-1 X-ray dipole at harder energies. The normalised amplitude of the ROSAT XRB dipole is  $\sim 1.6\%$ .

## Subtracting the Diffuse Galactic Emission

A major problem in extracting the X-ray background dipole at soft X-rays is the large contribution of our Galaxy at such energies (cf. Kneissl et al 1998). We attempt to model the diffuse Galactic component using a finite radius disk with an exponential scale height, (Iwan et al. 1982) which provides a good description of the Galactic component at harder energies (2-60 keV). The fit to the model is performed by excluding the regions of the most apparent extended Galactic emission features: the North Polar Spur and the  $|b| < 20^\circ$  strip as well as most apparent "local" extragalactic features; a  $4^\circ$  radius region around the Virgo cluster ( $l, b \approx 287^\circ, 75^\circ$ ) and a  $10^\circ$  radius region around the Magellanic clouds ( $l, b \approx 278^\circ, -32^\circ$ ).

We obtain a fraction of the total X-ray emission which is due to the Galaxy consistent with  $\sim 25\%$  while the disk scale height and disk radius were found to be 16 & 27 kpc respectively.

## Dipole Estimation

After excluding from the ROSAT counts our best fit Galactic model and after masking, using either of two methods; *homogeneous filling procedure* or a *spherical harmonic* extrapolation procedure, the following regions: (a) The Galactic plane, with  $|b| \leq 20^\circ$  or  $30^\circ$ , (b) the area dominated by the Galactic bulge and the North Polar Spur (ie.,  $-40^\circ < b < 75^\circ$  and  $300^\circ < l < 30^\circ$ ), (c) the Large Magellanic Clouds (ie., an area of  $10^\circ$  radius centred on  $l, b \approx 278^\circ, -32^\circ$ ), we measure the dipole by weighing the unit directional vector pointing to each  $40^2$  arcmin<sup>2</sup> ROSAT cell with the X-ray intensity  $\mathcal{C}_i$  of that cell. We normalize the dipole by the monopole term (the mean X-ray intensity over the sky):  $\mathcal{D} \equiv |\mathbf{D}|/M = \sum \mathcal{C}_i \hat{\mathbf{r}}_i / \sum \mathcal{C}_i$

## Dipole Results

When using the raw ROSAT data, the dipole points towards the Galactic centre (in agreement with the analysis of Kneissl et al 1997). However, when we exclude both the Galaxy and the North Polar Spur, the measured dipole is in much better directional agreement with the CMB dipole. For the *homogeneous filling* method we find  $\delta\theta_{cmb} \sim 20^\circ$  while for the *spherical harmonic* method the misalignment angle is larger,  $\delta\theta_{cmb} \sim 51^\circ$ .

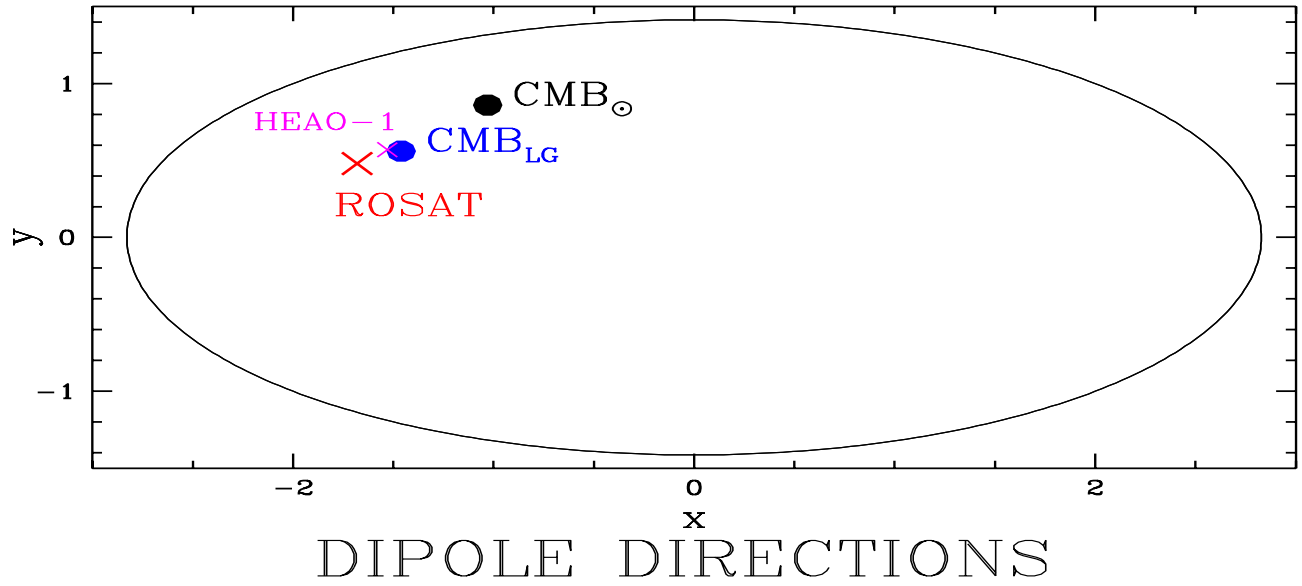
However, it should be expected that many Galactic sources, probably dominating the **higher ROSAT counts**, are still present in the data and could affect the behaviour of the estimated extragalactic XRB dipole. Excluding the highest  $\sim 3\%$  of the counts ( $\mathcal{C}_{up} \gtrsim 140$ ) we find that *both methods used to model the masked areas agree and the XRB-CMB dipole misalignment angle is reduced significantly*

The interpretation that the high intensity cells are associated with Galactic sources is supported by the fact that when we include these few cells the resulting dipole direction moves towards the Galactic centre.

Therefore, taking into account the variations of our results due to (a) the uncertainties of the Galactic model subtracted from the raw counts, (b) to the different methods used to mask the excluded sky regions and (c) to the different galactic latitude limits, we conclude that the *extragalactic* ROSAT dipole has:

$$\mathcal{D}_{\text{XRB,ROSAT}} \approx 0.016 \pm 0.008 \quad (l, b) \approx (288^\circ, 25^\circ) \pm 19^\circ$$

Our results are consistent with the HEAO-1 (2-10 keV) dipole (Shafer & Fabian 1983) which points in a similar direction ( $282^\circ, 30^\circ$ ) but has a lower amplitude:  $\mathcal{D}_{\text{XRB,HEAO-1}} \sim 0.005$ .



## References

- [1] Iwan D., Marshall F.F., Boldt E.A., Mushotzky R.F., Shafer R.A., & Stottlemeyer A., 1982, ApJ, 260, 111
- [2] Kneissl R., Egger R., Hasinger G., Soltan A.M. & Trumper J., 1997, AA, 320, 685
- [3] Lahav O., Piran T. & Treyer, M., 1997, MNRAS, 284, 499
- [4] Shafer R.A., Fabian A.C., in Abell G.O., Chincarini G., eds, IAU Symp. No 104, Dordrecht, p.33
- [5] Snowden S.L. et al, 1995, ApJ, 454, 643

# The Angular Correlation Function of RASS Extragalactic Sources

T. Akylas, M. Plionis & I. Georgantopoulos

Astronomical Institute, National Observatory of Athens,  
I.Metaxa & Bas.Pavlou, Lofos Koufou, 15236, Athens, Greece

We investigate the clustering properties of a new homogeneous sample of 2000 extragalactic sources selected from the ROSAT XRT/PSPC All-Sky survey (Voges *et al* 1996). Assuming that this sample is dominated by QSO's we find that the characteristic depth of the sample is  $\sim 410 h^{-1}$  Mpc. We find a significant angular correlation function, between  $\sim 2^\circ$  and  $15^\circ$  which roughly corresponds to a spatial correlation length of  $r_o \simeq 15.5 \pm 4.5 h^{-1}$  Mpc, roughly consistent with that of optically selected QSO's at  $\langle z \rangle \simeq 1.5$ .

## Method

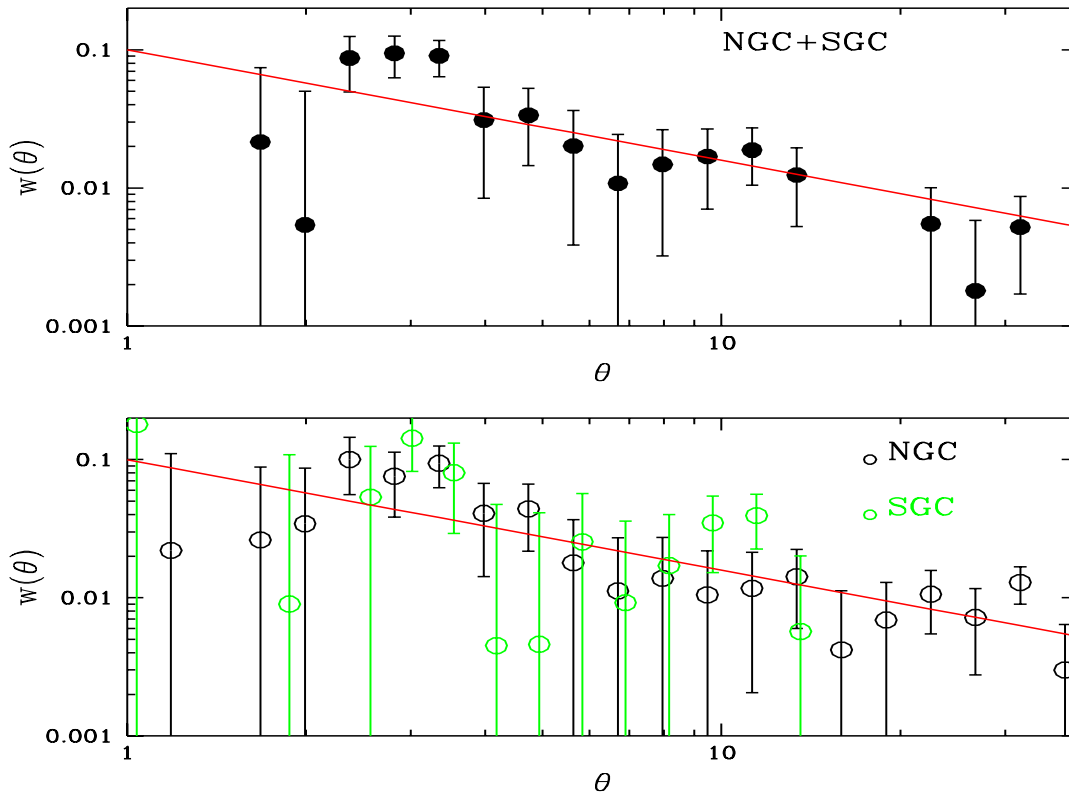
The original RASS sample contains 18811 sources which include stars and extragalactic sources over the entire 0.1 - 2 keV energy range. To exclude the stellar objects we cross correlated this sample with star catalogs (SAO, GSC, RASSOB, RASSWD, XRBCAT and CVCAT). Furthermore, we have cross-correlated the remaining sources (for  $b > 0^\circ$ ) with the Hamburg identifications (Bade *et al* 1998) to find that most of them, after excluding those with extension flag  $> 40$ , are identified as QSO's. In order to produce a homogeneous sample in exposure time we have omitted sources with count rate  $< 0.1$  which results in a homogeneous sample over 92% of the sky. Finally, we exclude regions heavily affected by Galactic absorption, ie.,  $|b| < 30^\circ$  as well as  $\delta < -30^\circ$  (see below). Our final catalogue contains 2000 extragalactic sources.

We further need to estimate the various selection functions that could affect the clustering properties of our survey. For example the significant absorption due to the diffuse Galactic Neutral Hydrogen could artificially enhance the 2-point correlation function and also introduce large-scale modulations. Therefore, we have cross correlated our RASS catalogue with the recent Leiden/Dwingeloo Atlas of Galactic Neutral Hydrogen (Hartmann & Burton 1997) which covers regions with  $\delta \geq -30^\circ$ , to derive the RASS surface density as a function of  $N_H$ , which is used to produce a random catalogue with similar absorption selection function.

## Results

The correlation function estimator we use is:  $w(\theta) = fN_{dd}/N_{dr} - 1$ , where the normalization factor is  $f = 2 \times N_r/N_o$ . Assuming a 2-p correlation function of the form  $w(\theta) = (\theta/\theta_o)^b$  we find  $b = -0.9 \pm 0.15$  and  $\theta_o = 0.08^\circ \pm 0.05^\circ$ .

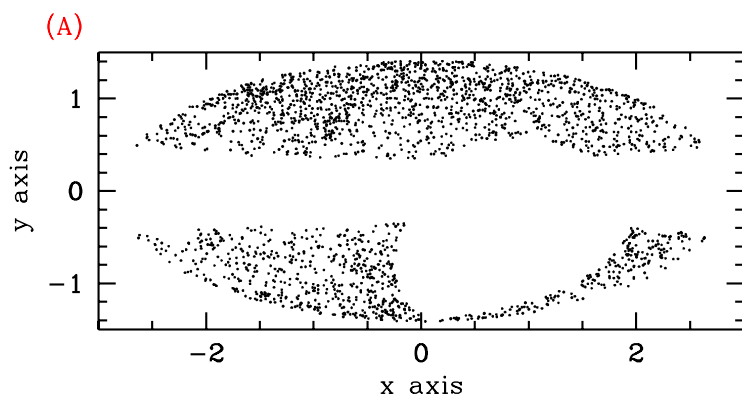
A preliminary calculation using the average flux limit ( $\sim 10^{-12}$  erg/sec  $\text{cm}^2$ ) of the RASS over the area used and a QSO characteristic luminosity of  $L_* \simeq 2 \times 10^{43}$  (Boyle *et al* 1993) gives a characteristic depth of  $D_* \sim 410 h^{-1}$  Mpc. Using Limber's equation to relate the angular and spatial 2-point correlation function with  $\gamma \simeq 2$  we find a correlation length of  $r_o \simeq 15.5 \pm 4.5 h^{-1}$  Mpc, which is compatible only with comoving QSO clustering (cf. Shanks & Boyle 1994 and La Franca *et al* 1998 which find  $r_o \simeq 10 \pm 2.5 h^{-1}$  Mpc at  $\langle z \rangle \simeq 1.5 - 1.8$ )



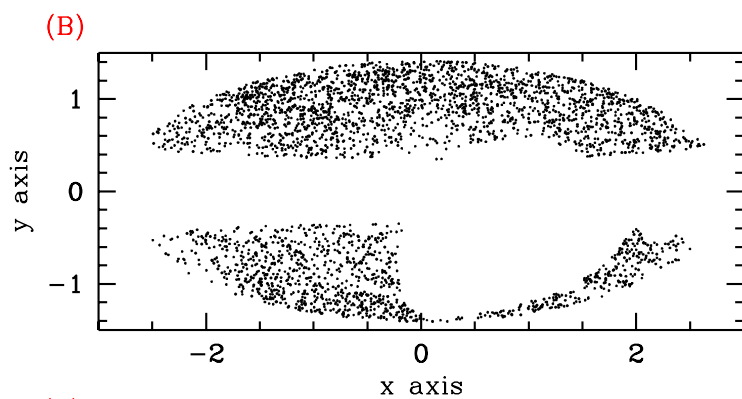
## References

- [1] N. Bade *et al*, 1998, A&AS, 127, 145
- [2] B.J. Boyle *et al*, 1993, MNRAS, 260, 49
- [3] F. La Franca, P. Andreani & S. Christiani, 1998, ApJ, 497, 529

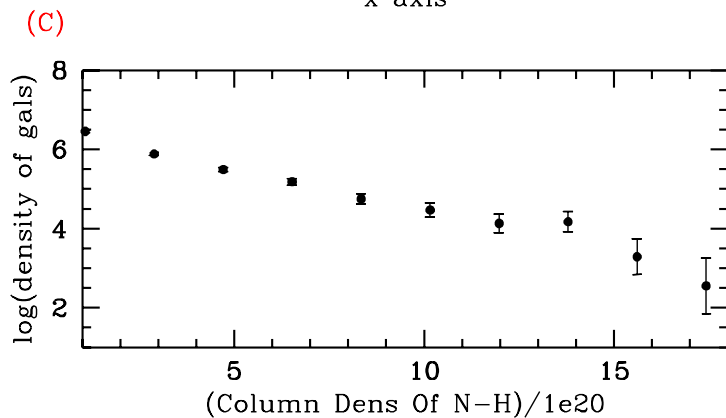
- [4] D.Hartmann & W.B.Burton, 'Atlas of Galactic Neutral Hydrogen', 1997, Cambridge Univ. Press.
- [5] T.Shanks & B.J.Boyle, 1994, MNRAS, 271, 753
- [6] W. Voges *et al.* 1996 IAU Circ., 6420, 2



Aitoff projection of the RASS extragalactic sources (N=2400), with  $|b| > 20$  and  $\text{dec} > -30$  deg.



Aitoff projection of a random catalog (N=3000), with  $|b| > 20$  and  $\text{dec} > -30$  deg based on Leiden/Dwingeloo N-H map.



Number of RASS galaxies per steradian as a function of N-H value.

# Galaxy Cluster Shapes

S. Basilakos<sup>1, 2</sup>, M. Plionis<sup>1</sup> & S. Maddox<sup>3</sup>

<sup>1</sup> Astronomical Institute, National Observatory of Athens,  
I.Metaxa & Bas.Pavlou, Lofos Koufou, 15236, Athens, Greece

<sup>2</sup> Section of Astronomy & Astrophysics, Univ. of Athens,  
Panepistimioupolis, 15784 Zografos, Athens, Greece

<sup>3</sup> Institute of Astronomy, Madingley Road, Cambridge, CB3 0EZ, UK

We study the performance of two different methods used to define cluster shapes with final aim to study the projected and intrinsic shapes of APM clusters (Dalton *et al* 1997). The **1<sup>st</sup>** method defines the cluster ellipticity by fitting ellipses to the individual galaxy distribution as a function of radius from the cluster centre. The **2<sup>nd</sup>** method is based on smoothing the discrete galaxy distribution and then fits an ellipse using all cells that fall above an overdensity threshold. This latter method is free of the known aperture bias which tends to artificially sphericalize clusters. Using Monte-Carlo simulations we have studied the performance of both methods in the presence of the expected galaxy background at the different distances traced by the APM clusters.

## The Method

In order to estimate the projected cluster shape we diagonalize the inertia tensor ( $\det(\mathbf{I}_{ij} - \lambda^2 \mathbf{M}_2) = 0$ ) where  $\mathbf{M}_2$  is the  $2 \times 2$  unit matrix. The eigenvalues  $(a, b)$  with  $(a > b)$  define the ellipticity of the configuration under study:  $\varepsilon = 1 - b/a$  (cf. Plionis, Barrow & Frenk 1991).

Initially all galaxy positions are transformed to the coordinate system of each cluster by  $x_i = (RA_g - RA_{cl}) \times \cos(\delta_{cl})$  and  $y_i = \delta_g - \delta_{cl}$ . Then we use the following procedures:

**1<sup>st</sup> Method:** All galaxies within an initial small radius are used to define the initial value of the cluster shape parameters. Then the next nearest galaxy is added to the initial group and the shape is recalculated. This method, although straight forward, suffers from the fact that implicitly we are assuming a spherical aperture within which the cluster shape parameters are estimated (cf. Binggeli 1982).

**2<sup>nd</sup> Method:** The discrete galaxy distribution is smoothed using a Gaussian kernel. Then all cells that have a density above some threshold are used to define the moments of inertia

with weight  $w_i = \rho_i - \langle \rho(z) \rangle / \langle \rho(z) \rangle$  where  $\langle \rho(z) \rangle = \int_{M_{min}(z)}^{M_{max}} \Phi(M) dM$  with  $\Phi(M)$  the APM luminosity function (with  $z$  evolution) from Maddox, Efstathiou & Sutherland (1996) and  $M_{min}(z) = m_{lim} - 5 \log(r) - 25 - 3z$ . This method is free of the aperture bias and we found that it performs significantly better than the previous method.

### Background Contamination

A major problem in reliably determining cluster shapes is the significant galaxy background which contaminates the cluster galaxy counts, especially in deep galaxy catalogues like the APM which has  $m_{lim} = 20.5$ . In order to assess the effects of such contamination on the determination of cluster shapes we have performed large sets of Monte-Carlo simulations in which we compared the determination of cluster shapes, defined to have the King's profile with core radii  $\leq 0.1 h^{-1}$  Mpc (cf. Girardi *et al* 1998), with and without the expected background contamination. The background at each cluster distance was estimated by:

$$N_{bac} = 2\pi(1 - \cos\theta^i) \int_0^{z_{max}} \langle \rho(z) \rangle z^2 dz$$

where  $\theta^i$  is the angular radius of the cluster. In the figure we show an example of a simulated cluster at  $200 h^{-1}$  Mpc with  $\varepsilon = 0.5$ . The performance of the two methods, described above, is shown in the same colour coding as in the text. It is evident that the 2<sup>nd</sup> method performs equally well in the presence or not of the galaxy background. However, the presence of substructure can affect unexpectedly the performance of this method as well.

We are at the process of quantifying biases related to the above methods and applying our shape determination procedure to the real APM data.

## References

- [1] B. Binggeli, 1982, A&A, 250, 432
- [2] G.B. Dalton *et al*, 1997, MNRAS, 289, 263
- [3] M. Girardi *et al.*, 1998, astro-ph/9804187
- [4] S. Maddox, G. Efstathiou, W.J. Sutherland, 1996, MNRAS, 283, 1227
- [5] M. Plionis, J.D. Barrow, C.S. Frenk, 1991, MNRAS, 249, 662

SIMULATED CLUSTER at 200  $h^{-1}$  Mpc with  $\epsilon=0.5$  & King's profile

